Diagn Interv Radiol 2022; 28:131–137

ABDOMINAL IMAGING

ORIGINAL ARTICLE

Relative contribution of susceptibility weighted imaging, compared to conventional MRI, in the detection of common bile-duct calculi

Vishal Singh
Jaladhar Neelavalli
Suhail P. Parvaze
Mamta Gupta
Radha K. Verma
Avnish K. Seth
Lakshay Mehta
Rakesh Kumar Gupta

PURPOSE
We aimed to evaluate the relative contribution of susceptibility weighted imaging (SWI) in the detection of common bile-duct (CBD) stones in comparison to the conventional MRI protocol containing magnetic resonance cholangiopancreatography (MRCP), balanced turbo field echo (BTFE), and T2-weighted spin-echo imaging techniques.

METHODS
MRI data containing MRCP, BTFE, T2-weighted imaging, and abdominal SWI were independently evaluated by 2 sets of experienced radiologists in 44 patients with confirmed CBD stones. Endoscopic retrograde cholangiopancreatography, and endoscopic ultrasound where available, was used as the reference gold standard. Evaluation was performed for the visualization of CBD stones in each of the MRI techniques. Relative contribution of SWI was classified into one of four categories for each case: (1) no contribution to CBD stone visualization; (2) same as conventional techniques; (3) improved diagnostic confidence; and (4) critical for diagnosis. Stone size was also assessed.

RESULTS
Inter-rater agreement coefficient for CBD stone visualization was found to be "good" in MRCP (0.77), "very good" in SWI (0.94) and BTFE (0.84), and moderate in T2-weighted imaging (0.54). CBD stones were visualized with SWI in 86.4% and 82%, with MRCP in 70.5% and 70.5% cases, with BTFE in 73% and 61.4% cases, with T2-weighted imaging in 45.5% and 52.3% cases by reviewers 1 and 2, respectively. SWI did not contribute to CBD stone visualization in 2.3% (1/44); was the same as conventional techniques in 31.8% (14/44) cases; improved diagnostic confidence in 34.1%; and was critical for diagnosis in 20.5% cases.

CONCLUSION
SWI has the potential to serve as a strong adjunct to conventional MRI protocols used for CBD stone evaluation with very small scan-time penalty.

Choledocholithiasis is one of the common complications of gallstone disease, which is also known as cholelithiasis. While primary stones form within the bile ducts, the secondary stones, which are most common, originate in the gallbladder and migrate through the cystic duct to the CBD, affecting the bile flow. Incidence of gallstone disease ranges from 15% to 22% in the world,[1,2] and about 5% to 20% of this population are found to have choledocholithiasis.[3] Patients with choledocholithiasis often present with right upper abdominal pain and/or jaundice. Clinical investigation of patients with suspected CBD stones involves laboratory tests for liver function and imaging.[4] Serum levels of bilirubin and alkaline phosphatase, together with blood levels of gamma-glutamyl transferase, are used for evaluating suspected CBD stone. While these liver function tests help in indicating the risk of CBD stone, they are nonspecific and hence are often followed by confirmatory imaging. Endoscopic retrograde cholangiopancreatography (ERCP) or endoscopic ultrasound (EUS) could be used for CBD stone evaluation. ERCP is both a diagnostic and therapeutic technique, and EUS is a diagnostic technique. However, both of them are invasive modalities. From a diagnostic perspective, ERCP is associated with the risk of complications, being an invasive procedure. EUS has high sensitivity (97%) and specificity (87%) in the detection of CBD stones.[5] However, being an endoscopic

From the Fortis Memorial Research Institute (V.S., M.G., R.K.V., A.K.S., L.M., R.K.G. ✉ rk.gupta@fortishealthcare.com, ✉ rakeshree1@gmail.com), Gurgaon, IndiaPhilips Innovation Campus (J.N., S.P.P.), Philips India Limited, Bengaluru, India.

Received 4 September 2020; revision requested 12 October 2020; last revision received 28 December 2020; accepted 25 January 2021.

DOI: 10.5152/dir.2022.20713

You may cite this article as: Singh V, Neelavalli J, Parvaze SP, et al. Relative contribution of susceptibility weighted imaging, compared to conventional MRI, in the detection of common bile-duct calculi. *Diagn Interv Radiol*. 2022;28(2):131-137.

procedure, EUS too is associated with similar risks as diagnostic ERCP. Within the noninvasive diagnostic imaging options, abdominal ultrasound (US) is the first line of investigation.[6] Unfortunately, sensitivity of US is highly operator-dependent and variable (13%-80%) in detecting CBD calculi.[6,7] Other noninvasive diagnostic imaging options include computed tomography (CT) and magnetic resonance cholangiopancreatography (MRCP). Among these, CT has a relatively moderate sensitivity of 69%-87%,[7-9] while MRCP has higher sensitivity than CT and US (81%-93.7%) and is relatively operator independent. However, MRCP's sensitivity drops to 51%-64% when CBD stones are of smaller size, <5 mm.[10-12] Hence, the technique for improved detection of CBD stones is a necessity. A recent study showed that magnetic susceptibility may be used for sensitive detection of calculi within the gallbladder using susceptibility weighted magnetic resonance imaging (SWI).[13] Here, the magnetic susceptibility property of the stones was used for its visualization in both the magnitude and phase component of the MRI signal. Briefly, SWI is a high resolution spoiled gradient echo (GRE) or gradient echo echo-planar MRI technique that utilizes both the magnitude and phase information of the MR signal. The theory behind susceptibility weighting and phase sensitivity can be found in the excellent review by Haacke et al.[14] Phase images provide the additional capability to distinguish diamagnetic vs. paramagnetic tissue in vivo due to their sensitivity to tissue magnetic susceptibility property. Furthermore, with better signal-to-noise ratio characteristics than magnitude images for susceptibility-causing structures,[15] phase images are highly sensitive in picking up even small susceptibility structures like micro-bleeds in the brain.[16] Gupta et al.'s[13] work shows that SWI provides similar capabilities while imaging biliary anatomy. Given that most biliary stones contain cholesterol, calcium salts, or calcium bilirubinate, all of which exhibit magnetic susceptibility effect to varying degrees,[13] we hypothesized that SWI may help in improved detection of CBD stones. Hence, as a first step in evaluating this hypothesis, in this preliminary study, we assessed the role of SWI in the detection of CBD calculi. Specifically, we evaluated the relative contribution of SWI in CBD stone evaluation, compared to conventional MRI techniques used.

Main points

- Susceptibility signature of the common bile duct stones can be visualized in magnitude and/or phase data of susceptibility weighted MRI in most cases.
- Phase signature of the common bile duct stones can be dia- or paramagnetic or mixed phase.
- Susceptibility signature could provide improved diagnostic confidence in common bile duct (CBD) stone detection, as an adjunct to conventional MRI protocol for CBD stone imaging, especially for small stones.

Methods

This retrospective study (study code 2018-010IP-22) was approved by the local institutional review committee. Abdominal SWI data was collected in consecutive patients, since May 1, 2017, as part of an ongoing study looking at SWI's relevance in imaging the biliary system. Adult patients receiving a diagnostic MRI for suspected biliary pathology, subsequent to a diagnostic US examination were included in this larger study. Patients who had contraindication to MRI due to metallic implants were excluded. As part of this study, informed consent was obtained from all the patients before MRI. The data collected in such manner was later retrospectively evaluated for CBD stone visualization, for the purposes of the current study.

For the current retrospective evaluation study, inclusion criteria were: (a) patients receiving abdominal MRI exam between May 1, 2017, and March 15, 2020; (b) patients clinically suspected of having biliary stones or biliary pancreatitis, based on symptoms and abnormal liver function tests—alkaline phosphatase and gamma-glutamyl transferase levels; (c) patients who had received a subsequent ERCP with or without clinical EUS examination. Exclusion criteria were: (a) patients whose MRI scans were incomplete due to claustrophobia or other reasons.

All MRI examinations were performed on an Ingenia 3.0T (Philips) system. Imaging protocol consisted of the conventional diagnostic imaging sequences that included MRCP, T2- weighted BTFE and T2-weighted turbo spin echo, and an additional abdominal SWI, acquired with the imaging parameters shown in Table 1. Acquisition time for the 3D SWI in axial orientation was 17 s per breath-hold and consisted of 2-3 such breath-holds for covering the region of interest. Findings from diagnostic/therapeutic ERCP/EUS in the same sitting were used as gold standard to confirm MRI findings. Based on ERCP/EUS results, data of cases without CBD stones were excluded. The remaining data were reviewed by 2 radiologists with 9 and >30 years of experience in abdominal radiology, in consensus, denoted by cR for consensus review. These radiologists were blinded to the results of ERCP/EUS examination at the time of their review of MRI data. Both susceptibility weighted magnitude and the phase output from SWI sequence were reviewed as part of SWI data evaluation. Visualization status of calculi within a particular sequence data was noted as yes/no. The proportion of cases where calculi were visualized in conventional techniques (MRCP, balanced turbo field echo [BTFE], and T2-weighted imaging)) and in SWI were noted. In cases where stones were visualized in SWI, the nature of their phase signature was also measured as either diamagnetic (+ve phase), paramagnetic (–ve phase), or indeterminate (mixed phase).

The relative contribution of SWI was assessed by cR alone, and classified into one of four categories for each case: (1) no contribution to CBD stone visualization—defined as non-visualization of the CBD stone in SWI data, which was (were) clearly observed in at least one of the conventional techniques; (2) same as conventional techniques—defined as visualization of stones in SWI, which is in agreement, in location and extent, with one or more of the conventional techniques; (3) improved diagnostic confidence—defined as cases in which unambiguous visualization of stones in SWI (either phase or magnitude), which were only seen as suspicious duct narrowing, sludge, or filling defects in either of the 3 conventional techniques; (4) critical for diagnosis of CBD calculi—defined as cases in which there was clear visualization of stone(s) in SWI data (either phase or magnitude), which were missed in the first review of the data from conventional techniques.

Table 1. Summary of the typical imaging protocol with imaging parameters

Sequence	TR (ms)	TE (ms)	Bandwidth (Hz/pixel)	ETL or EPI factor	Flip angle (degrees)	Resolution (mm^3)
T2w_SPAIR	816	70	639	60	90	0.8 × 0.8 × 5
MRCP_2D	5703	692	425	256	90	0.6 × 0.6 × 60
MRCP_3D	1006	600	262	120	90	0.6 × 0.6 × 2
T2w_TSE_coronal	782	80	527	57	90	0.75 × 0.75 × 5
BTFE_SPIR	3.14	1.6	1141	144	90	1.14 × 1.14× 5 or 6
SWI	12	7.2	255	1	8	1 × 1 × 6

TR, repetition time; TE, echo time; ETL, echo train length; EPI, echo-planar imaging; T2w_SPAIR, T2-weigthed spectral attenuated inversion recovery; MRCP_2D/3D, magnetic resonance cholangiopancreatography two/three dimensional; TSE, turbo spin echo; BTFE_SPIR, balanced turbo field echo spectral presaturation with inversion; SWI, susceptibility weighted imaging.

Proportion of cases falling into each of the above mentioned categories was noted for assessing the relative contribution of SWI in the diagnosis of CBD stones. The size of the calculi was also evaluated, wherever possible, from the MRCP data. In case of multiple calculi, the smallest size of the calculi was measured. Sizes of the calculi were not determined from SWI data due to the confounding influence of the blooming effect.

For ruling out bias in stone visualization assessment, imaging data was independently reviewed by an additional radiologist with 20 years of experience in body imaging —denoted by R2 for second review. The radiologist was blinded to the diagnosis from ERCP/EUS. Inter-rater agreement between the 2 reviews was assessed using Gwet's agreement coefficient 1 (AC1 or γ).[17,18] Statistical analysis was performed on R package version 4.0.2[19] with significance value set at $P = 0.05$. Interpretation of the γ value was set as follows: $\gamma < 0.2$ poor agreement, $0.2 < \gamma < 0.4$ fair agreement, $0.4 < \gamma < 0.6$ moderate agreement, $0.6 < \gamma < 0.8$ good agreement, and $0.8 < \gamma < 1$ very good agreement.[20]

Results

A total of 51 patients, with clinically and biochemically suspected biliary calculi, who had an ERCP (and EUS, where available) and a complete MRI examination, were included in the study. Of these, 1 patient had multiple stones in the left hepatic duct and an additional 4 patients showed biliary sludge, which was confirmed on ERCP. Additionally, 1 patient had a CBD mass and 1 patient had a biliary stent, which precluded appropriate MRI-based assessment. No CBD calculi were found in these cases. These 7 subjects were hence excluded from image review by radiologists. Thus, n = 44 cases with CBD stones, confirmed by ERCP (and EUS, where available), were reviewed as part of this study.

In 5 of 44 cases, no stones were visualized in any of the MRI sequences. In consensus review, stones were visualized in 31/44 cases with MRCP (70.5%), 32/44 cases with BTFE (73%), 20/44 cases with T2-weighted imaging (45.5%), and 38/44 cases with SWI (86.4%). Among these cases, SWI was found to provide the same information as conventional imaging techniques in 31.8% (14/44); improve diagnostic confidence in 34.1% (15/44); be critical for diagnosis in 20.5% (9/44) of the cases; and not contribute to CBD stone visualization in 1 case, 2.3% (1/44).

According to the second independent reviewer, stones were visualized in 31/44 cases with MRCP (70.5%), in 27/44 cases with BTFE (61.4%), in 23/44 cases with T2-weighted imaging (52.3%), and in 36/44 cases with SWI (81.8%). Inter-rater agreement between cR and R2 was found to be good for MRCP ($\gamma = 0.77$, $P < .001$), very good for BTFE ($\gamma = 0.84$, $P < .001$), moderate for T2-weighted imaging ($\gamma = 0.54$, $P < .001$), and very good for SWI ($\gamma = 0.94$, $P < .001$). In one case, both reviewers visualized the calculi in SWI data alone, which was entirely missed in the data from other sequences. In the analysis by R2, stones were only visualized in SWI data in one additional case.

Size of the stones could be evaluated in 32 of the cases where they were visualized and measurable from MRCP. In some of these cases, stones were visualized in MRCP in retrospect, after their identification in SWI. In cases where SWI was found "critical for diagnosis", stone size could be assessed in 5 cases and the average stone size was found to be 3.4 ± 0.75 mm (mean ± standard deviation). In cases where SWI provided improved diagnostic confidence, average stone size, measured in 13 of the cases, was found to be 4.6 ± 0.96 mm, and in cases where SWI provided same information as conventional sequences, average stone size, in 14 cases, was measured to be 7.9 ± 3 mm.

Figures 1-4 show the images from representative cases where SWI data was critical for diagnosis (Figure 1); improved diagnostic confidence (Figure 2); provided same information as conventional imaging techniques (Figure 3); and did not visualize the stone (Figure 4). Figures 1-3 demonstrate clear visualization of the susceptibility signature of the stones in SWI images, especially in the phase images. Among the 38 cases where stones were visualized in SWI, 25 cases demonstrated mixed phase, 12 cases demonstrated diamagnetic phase, and 1 case demonstrated paramagnetic phase.

Discussion

This study evaluated the contribution of SWI in the diagnosis of CBD stones, relative to the conventional MRI techniques, which include MRCP, BTFE, and T2-weighted imaging. Magnetic susceptibility property of the tissue leads to both local and non-local magnetic field perturbations. These effects are visualized with high sensitivity by GRE phase images and in the high resolution T2* weighted magnitude images of SWI. Given the presence of susceptibility-causing constituents in biliary stones, it was hypothesized that SWI may have a role in sensitive visualization of CBD stones. Indeed, we found that in about 54.6% of the cases, information from SWI data contributed to the diagnostic identification of CBD calculi. Furthermore, in approximately 1 out of 5 cases (20.5%), information from SWI was critical for diagnosis. In these latter cases, calculi were often first noticed in SWI and were later identified in the other sequences, after careful re-evaluation. While SWI technique provides susceptibility weighted magnitude and filtered phase outputs, SWI phase images were the key

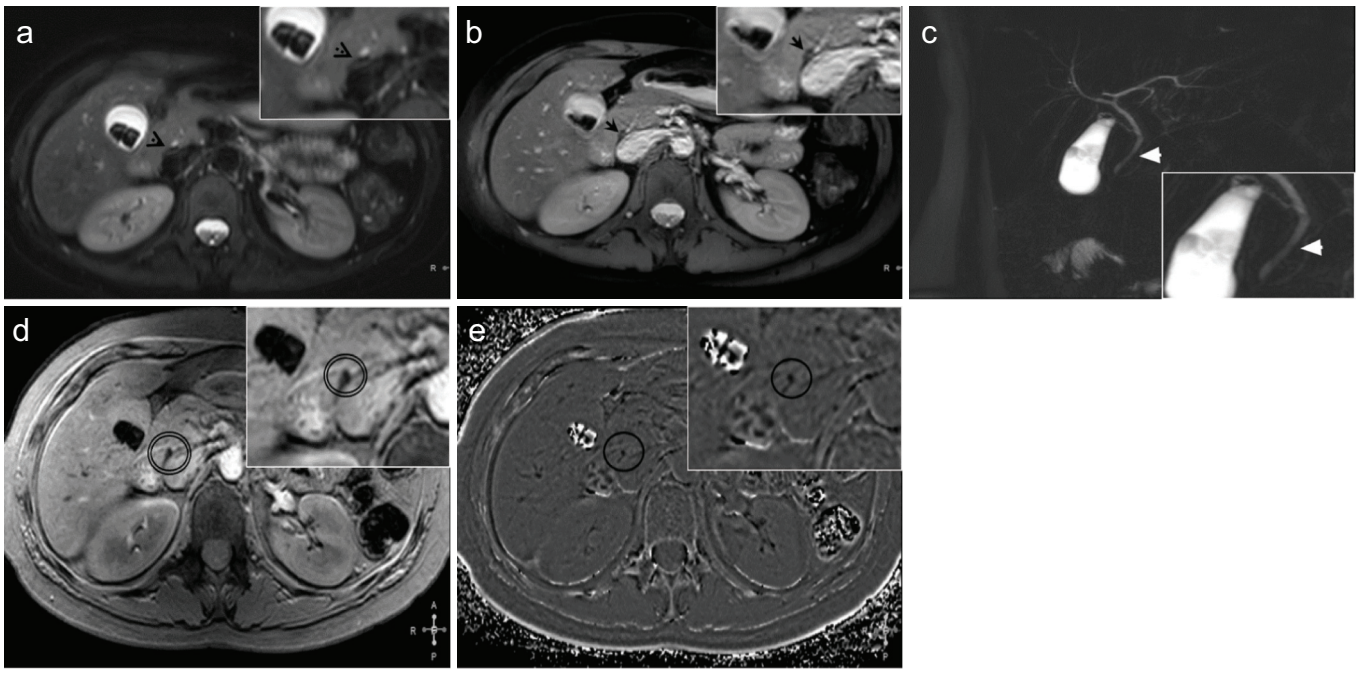

Figure 1. a-e. SWI critical for diagnosis—comparative collage of images from the same anatomical level, from one of the patients where SWI data was critical for diagnosis of identifying the CBD stone. T2-weighted imaging (**a**) and BTFE (**b**) are inconclusive in indicating the presence of calculus, while MRCP (**c**) indicates filling defect and possible sludge. In comparison, SWI data (**d, e**) clearly demonstrate the calculus (*circled*) with hypointense signal in magnitude (**d**) and negative phase signal in the corresponding region of the phase image (**e**).

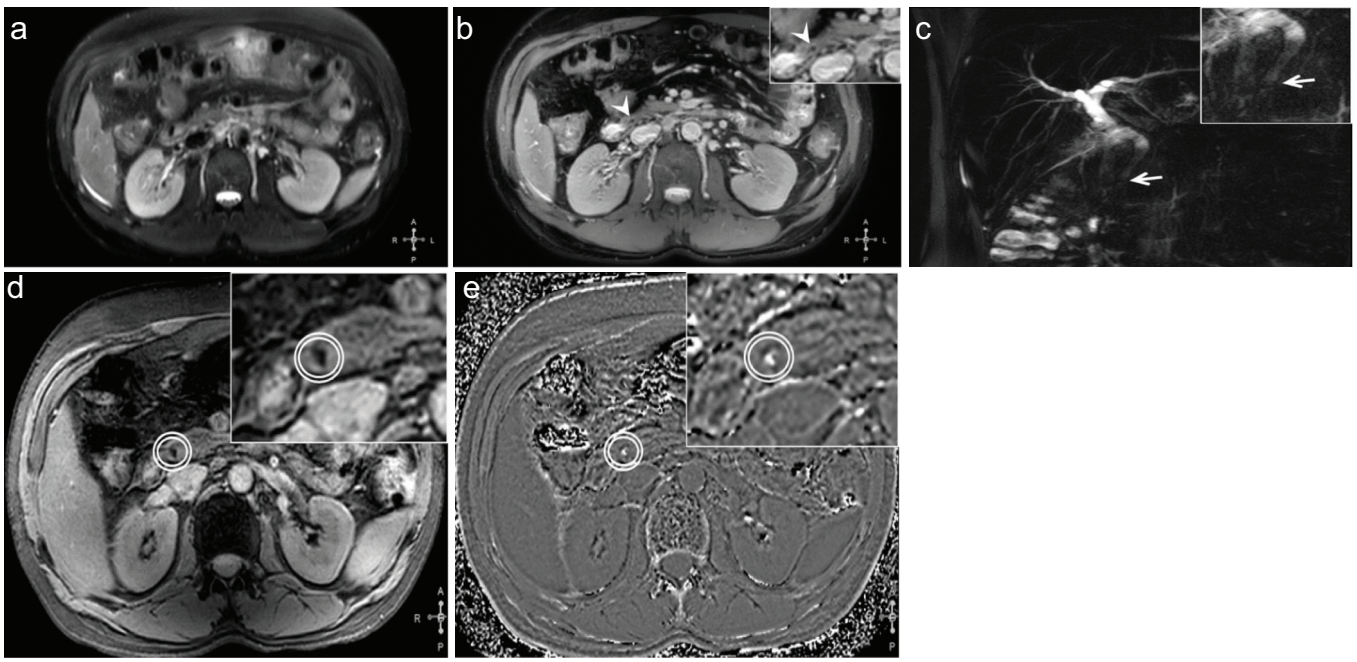

Figure 2. a-e. SWI improved diagnostic confidence—comparative collage of images from the same anatomical level, from one of the patients where SWI data provided improved diagnostic confidence for CBD stone identification. T2-weighted image (**a**) is not indicative. BTFE (**b**) indicates possible calculus, and MRCP (**c**) data indicates a filling defect and possible sludge. In comparison, SWI data (**d, e**) clearly demonstrated the calculus with hypointense signal in magnitude and hyperintense signal in phase (**e**) images in the corresponding region.

in stone identification. It is noteworthy that in 5 cases, while calculi were detected with ERCP, they were not visualized in MRI examination. This indicates that there is still room for improving the sensitivity of MRI in CBD calculus detection. In a small fraction of the cases where stones were visualized with MR (in 2.3%, 1/44 by cR; and in 4.6%, 2/44 by R2).

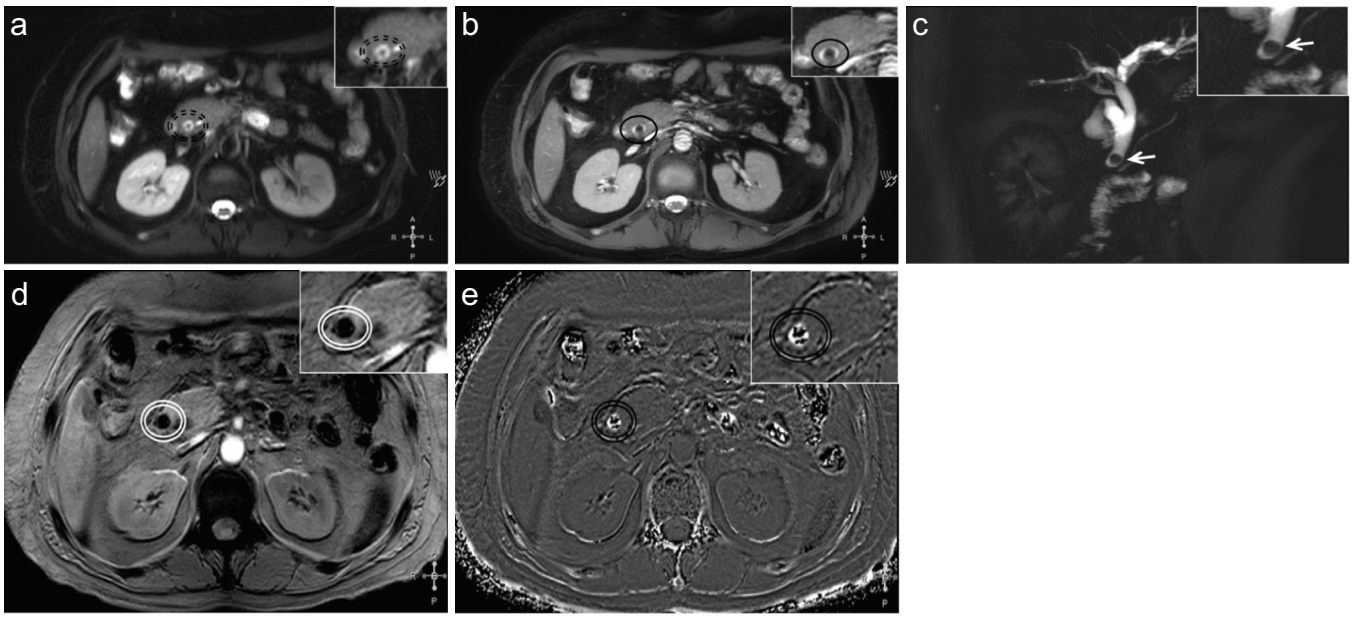

Figure 3. a-e. SWI was same as conventional techniques—comparative collage of images from the same anatomical level, from one of the patients where SWI data provided information same as conventional techniques in identifying CBD stone. T2-weighted (**a**), BTFE (**b**), and MRCP (**c**) clearly indicate the presence of a calculus in the same location. Similarly, SWI data demonstrate the calculus with hypointense signal in magnitude (**d**) and mixed phase signal in the phase image (**e**) in the corresponding region.

It is interesting to note that SWI had better success in detecting CBD stones (38/44, 36/44) compared to MRCP (31/44, 31/44) in both cR and R2, respectively. This is indeed a welcome, yet surprising result. This may be explained based on the different signal mechanisms behind their identification in MRCP vs. SWI. In MRCP, the lack (void) of MRI signal from the stone (due to lack of labile hydrogen protons), against the bright signal of the bile fluid, is the key to their identification. On the other hand, visualization in SWI phase is reliant on the magnetic susceptibility property of the stones, which is non-local and can affect MRI signal across a much larger spatial extent than the stone's dimensions. Due to this property, SWI is found to be most sensitive in identifying susceptibility-causing structures of even sub-voxel dimensions like micro-hemorrhages or venules.[21-23] The same property may enable better identification of CBD stones in SWI. This hypothesis is in-part supported by the finding that the mean stone size in cases where SWI was critical for diagnosis was almost half the stone size detected by using conventional sequences. Magnetic susceptibility of biliary stones has been found to be of similar order of magnitude as that of deoxygenated blood in a recent study,[13] adding further credence to SWI's increased sensitivity hypothesis. Susceptibility signature of most of the stones was mixed, as opposed to an earlier study[13] where most stones observed in the gall bladder were diamagnetic. Nevertheless, in this study too, cases with stones of diamagnetic phase signature (hyperintense phase) were far greater in number than those with paramagnetic phase. This is in line with the fact that most of the biliary stones contain cholesterol or calcium salts, which are diamagnetic.[13] A point to note here is the means of identifying dia- vs. paramagnetic structures in SWI phase images (ie, their appearance) differ from manufacturer to manufacturer, depending on whether they use left-handed or right-handed MRI systems.[24] In the Philips system used in this study, which has a right-handed MRI system, diamagnetic structures appear on hyperintense phase and paramagnetic ones appear on hypointense phase. The opposite is applicable for left-handed MRI systems like the one used by GE (General Electric Healthcare). Table 2 shows the acronyms used for the SWI technique by different vendors.

In this study, we also found that the sensitivities of MRCP and BTFE were comparable, by both reviewers, in CBD stone detection. This finding is broadly in line with recent in vivo and ex vivo studies, which found that gradient echo technique showed similar or higher sensitivity than MRCP for biliary stone detection.[25-27] In fact, adding gradient echo sequence to the protocol provided improved sensitivity toward stone detection. Of note, both BTFE and SWI are gradient echo techniques; however, SWI fared better than BTFE in stone detection. This may be, again, due to the phase information and also the longer echo times (relative to BTFE) used in SWI, which renders higher sensitivity to susceptibility structures than BTFE.

One case of CBD calculus was not visualized in SWI, by both cR and R2 in SWI. Two additional cases of calculi were not visualized in SWI by R2. This discordance between the reviewers could be due to various factors—which include, but are not limited to, differences in the way SWI phase data is read, low or imperceptible phase changes or ambiguous phase, which may be confounded with surrounding tissue boundaries. Indeed, in consensus review, the phase signature in these 2 additional cases was noted as being mixed. Lack of phase signature is also possible and was observed in the case where CBD calculus was missed by both reviewers. Interestingly, we observe that also sludge does not display a phase signature in filtered phase images of SWI. Similarly, Gupta et al.,[13] found that polyps and gallbladder nodules do not display any phase signature. Figure 4 illustrates the case from this study where no signal changes or susceptibility signature was observed for the CBD stone in SWI data, while the same was visualized as hypointense region in the duct in conventional techniques of T2-weighted imaging and BTFE. This may

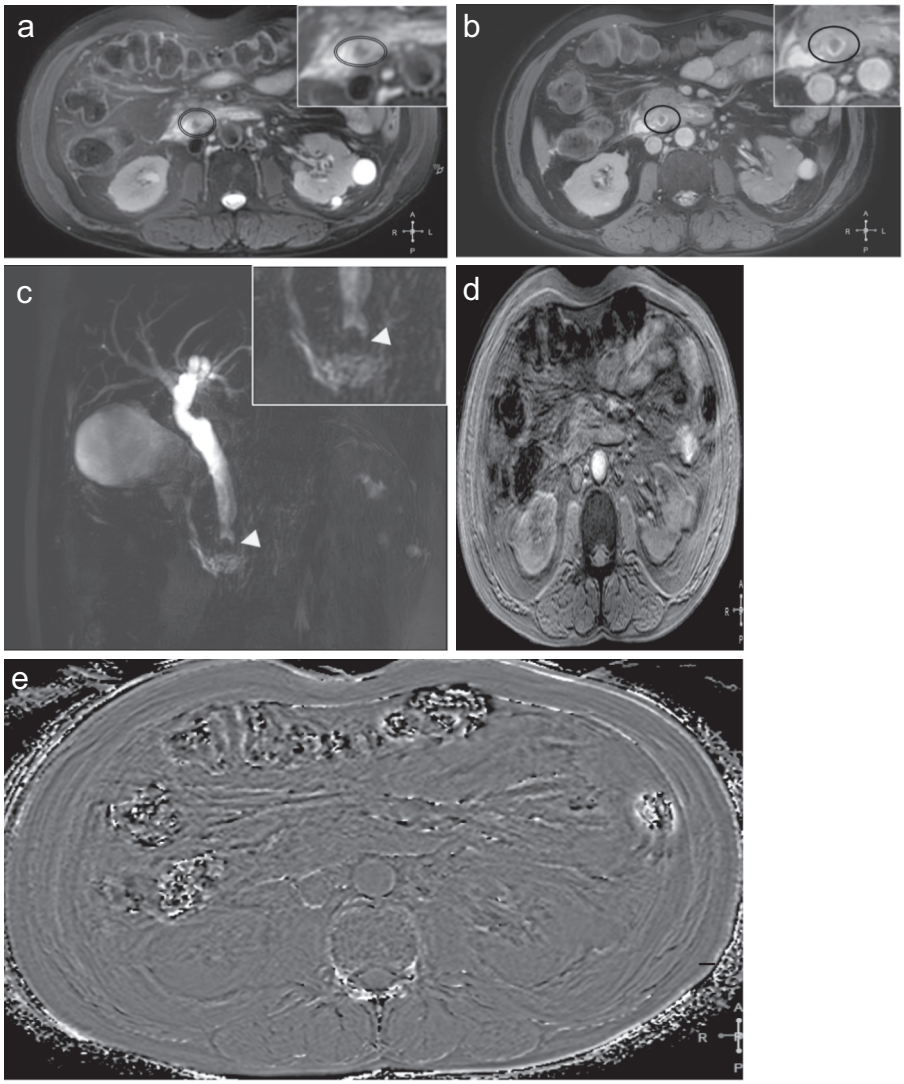

Figure 4. a-e. Stone not visualized in SWI—comparative collage of images from the same anatomical level, from one of the patients where the CBD stone was not visualized in SWI data. T2-weighted (**a**), BTFE (**b**), and MRCP (**c**) images indicated the presence of a calculus in the same location. SWI data, magnitude (**d**) and phase (**e**) images, do not show signal changes or susceptibility signature in the corresponding region. This may be because of slight motion blurring that is seen in the SWI data.

Table 2. Vendor acronyms for susceptibility weighted imaging

Vendor	Acronym
Siemens	SWI—Susceptibility weighted imaging
GE	SWAN—Susceptibility weighted angiography
Philips	SWIp—Susceptibility weighted imaging with phase
Canon	EFSBB—Enhanced flow-sensitive black blood
Hitachi	BSI—Blood-sensitive imaging

be due to the relatively short/intermediate TE used for SWI in this study, or due to very low magnetic susceptibility (relative to the surrounding tissue) of the calculus. One of the challenges in using SWI in the abdomen is the blooming artifacts from air-filled intestines, which are often adjacent to the CBD. While such blooming artifacts may be of diagnostic help in identifying pneumobilia in some cases,[28,29] it may also interfere with the ability to observe the duct. A breath-hold, single echo SWI technique with a reasonably short/intermediate TE of 7.2 ms was used in this study. A longer TE may have provided increased sensitivity to susceptibility structures, but at the expense of more artifacts from air-filled intestines. On the other hand, a shorter TE could have helped in reducing the blooming artifacts, at the expense of reduced sensitivity to susceptibility structures. Upon initial experimentation with a shorter and a TE longer than 7.2 ms, the intermediate value of 7.2 was empirically chosen for this study as it provided a reasonable balance between artifacts and sensitivity to susceptibility structures like biliary stones. Nevertheless, the intermediate TE may have limited our sensitivity to smaller and/or low magnetic susceptibility stones.

While this is the first study on the applicability of susceptibility weighted contrast for the evaluation of CBD stones, it has a few shortcomings. The study sample size is small, which has limited the power of the study. Measurement of the CBD stones could not be done from ERCP or EUS due to logistic reasons. Hence, size of the stones was measured from MRCP data. Furthermore, in cases where multiple stones were present, visualization in SWI was assessed for the smallest stone and not for each individual calculus due to the thick slices used in SWI (6 mm). The study design involved blinded review of, ERCP confirmed (and EUS, where available), CBD stone-containing cases alone. It may have been appropriate to include all 51 cases suspected of having CBD calculi in the MRI data analysis. However, given that the focus of this preliminary study was to assess SWI's role in CBD stone detection, we thought it to be appropriate to focus on cases that had confirmed CBD calculi. Furthermore, MRI data review and analysis was performed with a view to evaluate how SWI fares compared to conventional techniques in an unblinded manner, ie, findings from conventional MRI techniques were kept in view during the review of SWI data and *vice versa*. Despite the study design, we did find that in about one-fifth of the cases, findings in SWI were critical for diagnosis, and in one case, SWI was the only technique where CBD stone was visualized by both reviewers. Furthermore, the 2 results—highest inter-rater agreement of SWI and high sensitivity of SWI for CBD stone detection (noted by both reviewers)—when taken together, indicate the positive contribution of SWI in improved diagnosis of CBD calculi.

In conclusion, we find that SWI has the potential to serve as a strong adjunct to conventional MRI protocols used for CBD stone evaluation with very small scan-time penalty.

Conflict of interest disclosure

The authors declared no conflicts of interest.

References

1. Zhang W. Epidemiology and risk factors of cholelithiasis. *J Surg Concepts Pr*. 2011;16:408-412.
2. Shaffer EA. Epidemiology and risk factors for gallstone disease: Has the paradigm changed in the 21st century? *Curr Gastroenterol Rep*. 2005;7(2):132-140. [Crossref]
3. Everhart JE, Ruhl CE. Burden of Digestive Diseases in the United States Part III: Liver, Biliary Tract, and Pancreas. *Gastroenterology*. 2009;136(4):1134-1144. [Crossref]
4. Giljaca V, Gurusamy KS, Takwoingi Y, et al. Endoscopic ultrasound versus magnetic resonance cholangiopancreatography for common bile duct stones. *Cochrane Database Syst Rev*. 2015;5(2):118.
5. Manes G, Paspatis G, Aabakken L, et al. Endoscopic management of common bile duct stones: European Society of Gastrointestinal Endoscopy (ESGE) guideline. *Endoscopy*. 2019;51(5):472-491. [Crossref]
6. JJ C. US Diagnosis of choledocholithiasis: A reappraisal. *Radiology*. 1986;161(1):133. [Crossref]
7. Kondo S, Isayama H, Akahane M, et al. Detection of common bile duct stones: Comparison between endoscopic ultrasonography, magnetic resonance cholangiography, and helical-computed- tomographic cholangiography. *Eur J Radiol*. 2005;54(2):271-275. [Crossref]
8. Anderson SW, Lucey BC, Varghese JC, Soto JA. Accuracy of MDCT in the diagnosis of choledocholithiasis. *AJR Am J Roentgenol*. 2006;187(1):174-180. [Crossref]
9. Chen W, Mo JJ, Lin L, Li CQ, Zhang JF. Diagnostic value of magnetic resonance cholangiopancreatography in choledocholithiasis. *World J Gastroenterol*. 2015;21(11):3351. [Crossref]
10. Zidi SH, Prat F, Le Guen O, et al. Use of magnetic resonance cholangiography in the diagnosis of choledocholithiasis: Prospective comparison with a reference imaging method. *Gut*. 1999;44(1):118. [Crossref]
11. Jendresen MB, Thorbøll JE, Adamsen S, Nielsen H, Grønvall S, Hart-Hansen O. Preoperative routine magnetic resonance cholangiopancreatography before laparoscopic cholecystectomy: A prospective study. *Eur J Surg*. 2002;168 (12):690. [Crossref]
12. Gandhi D, Ojili V, Nepal P, et al. A pictorial review of gall stones and its associated complications. *Clin Imaging*. 2020;60(2):228-236. [Crossref]
13. Gupta RK, Neelavalli J, Gupta M, et al. Evaluation of gall bladder stones using susceptibility weighted imaging. *J Comput Assist Tomogr*. 2019;43(5):747-754. [Crossref]
14. Haacke EM, Tang J, Neelavalli J, Cheng YCN. Susceptibility mapping as a means to visualize veins and quantify oxygen saturation. *J Magn Reson Imaging*. 2010;32(3):663-676. [Crossref]
15. Duyn JH, Van Gelderen P, Li TQ, De Zwart JA, Koretsky AP, Fukunaga M. High-field MRI of brain cortical substructure based on signal phase. *Proc Natl Acad Sci U S A*. 2007;104 (28):11796. [Crossref]
16. Haacke EM, Xu Y, Cheng YCN, Reichenbach JR. Susceptibility weighted imaging (SWI). *Magn Reson Med*. 2004;52(3):612-618. [Crossref]
17. Gwet KL. Computing inter-rater reliability and its variance in the presence of high agreement. *Br J Math Stat Psychol*. 2008;61(Pt-1):29-48. [Crossref]
18. Wongpakaran N, Wongpakaran T, Wedding D, Gwet KL. A comparison of Cohen's Kappa and Gwet's AC1 when calculating inter-rater reliability coefficients: A study conducted with personality disorder samples. *BMC Med Res Methodol*. 2013;13(1):61. [Crossref]
19. R Core Team. R: A Language and Environment for Statistical Computing [Internet]. Vienna, Austria; 2020. Available from: https://www.r-project.org/.
20. Gwet KL. *Handbook of Inter-Rater Reliability: The Definitive Guide to Measuring the Extent of Agreement among Raters*. Gaithers burg, MD: STATAXIS Publishing Company; 2010.
21. Reichenbach JR, Venkatesan R, Schillinger DJ, Kido DK, Haacke EM. Small vessels in the human brain: MR venography with deoxyhemoglobin as an intrinsic contrast agent. *Radiology*. 1997;204(1):272-277. [Crossref]
22. Nandigam RNK, Viswanathan A, Delgado P, et al. MR imaging detection of cerebral microbleeds: Effect of susceptibility-weighted imaging, section thickness, and field strength. *Am J Neuroradiol*. 2009;30(2):338-343. [Crossref]
23. Nair JR, Van Hecke W, De Belder F, et al. High-resolution susceptibility-weighted imaging at 3 T with a 32-channel head coil: Technique and clinical applications. *AJR Am J Roentgenol*. 2010;195(4):1007-1014. [Crossref]
24. Mehemed TM, Yamamoto A. High-pass-filtered phase image: Left-versus right-handed MR imaging systems. *AJNR Am J Neuroradiol*. 2013;34:E72. [Crossref]
25. Erden A, Haliloğlu N, Genç Y, Erden İ. Diagnostic value of T1-weighted gradient-echo in-phase images added to MRCP in differentiation of hepatolithiasis and intrahepatic pneumobilia. *AJR Am J Roentgenol*. 2014;202 (1):74-82. [Crossref]
26. Kim YK, Kim CS, Lee JM, et al. Value of adding T1-weighted image to MR cholangiopancreatography for detecting intrahepatic biliary stones. *AJR Am J Roentgenol*. 2006;187(3): W267–74. [Crossref]
27. Tsai HM, Lin XZ, Chen CY, Lin PW, Lin JC. MRI of gallstones with different compo sitions. *AJR Am J Roentgenol*. 2004;182(6):1513-1519. [Crossref]
28. Kania L, Guglielmo F, Mitchell D. Interpreting body MRI cases: Classic findings in abdominal MRI. *Abdom Radiol*. 2018;43(10):2790. [Crossref]
29. Prabhakar PD, Prabhakar AM, Prabhakar HB, Sahani D. Magnetic resonance cholangiopancreatography of benign disorders of the biliary system. *Magn Reson Imaging Clin N Am*. 2010;18(3):497-514. [Crossref]